AUT Journal of Mechanical Engineering

AUT J. Mech. Eng., 7(3) (2023) 241-260
DOI: 10.22060/ajme.2024.22382.6064

Mathematical study on performance enhancement of solar updraft tower power plant by hot gas injection from an external source

M. Setareh [1,2]*, M. R. Assari [1,2]

[1] Jundi-Shapur Research Institute, Jundi-Shapur University of Technology, Dezful, Iran
[2] Department of Mechanical Engineering, Jundi-Shapur University of Technology, Dezful, Iran.

ABSTRACT: In this paper, a theoretical model for simulation of a solar updraft tower power plant with the assumption of axisymmetric condition is developed to study the impact of hot gas injection at the chimney base as well as extraction of a portion of hot gas after the turbine and re-entered it at the collector inlet. A new computational code is written by Matlab software and the effects of operational parameters are studied. Results show that the maximum power output is increased by 49.9% by increasing the extraction fraction from 0% to 40% at a wind velocity of 10 m/s. Besides, the obtained results show that the power output is enhanced as the mass flow rate of hot gas increases. As a result, the maximum power output at a hot gas mass flow rate of 30 kg/s is approximately 37% higher than the one at a hot gas mass flow rate of 10 kg/s. Results reveal that the optimum performance of SUTPP takes place at the ratio of pressure drop across the turbine to driving pressure potential in the range from 0.83 to 0.87. Furthermore, the power output in the presence of wind is investigated and the positive influence of wind is illustrated. Results indicate that by increasing the wind velocity from 10 m/s to 30 m/s, the maximum power output is increased by 386.1%.

Review History:

Received: May, 04, 2023
Revised: Jan. 09, 2024
Accepted: Jan. 13, 2024
Available Online: Jan. 16, 2024

Keywords:

Theoretical model
Solar updraft tower power plant
Hot gas injection
Driving pressure potential
Wind

1- Introduction

In recent decades, the rapid growth of energy consumption and restricting regulations of using fossil fuels in many countries due to destructive effects such as global warming, greenhouse impact, climate changes, acid rain, carbon dioxide emission, etc., the necessity of fossil fuel consumption reduction and the development and use of renewable energies are inevitable. Renewable energies include various kinds of sources that come from natural, available, and sustainable resources such as the sun, wind, etc. The development of renewable energies leads to technological progress as well as various economic and social benefits in the world. Different kinds of renewable energy systems have been introduced by researchers regarding the available resources in different geographical areas. Solar chimney power plant (SCPP) or solar updraft tower power plant (SUTPP) is one of the most interesting ways to generate electricity from solar energy. A SUTPP mainly consists of a transparent collector, turbine, and chimney. Fig. 1 shows the schematic diagram of a SUTPP system. The collector ceiling is covered by glass or transparent plastic and the ground surface is considered as an absorber at the collector floor.

The incident solar radiation on the collector is transmitted from the collector cover and absorbed by the ground and consequently, the temperature of the ground is raised. Heat is transferred by the convection mechanism to the air inside the collector and warm air is moved toward the chimney due to buoyancy force because of density difference and the greenhouse effect. The heated air inside the collector is moved upward to drive the turbine mounted at the chimney base and is discharged into the environment at the chimney outlet.

The idea and description of SUTPP system were first introduced in 1931 [1]. The first 50 kW SUTPP prototype was built in Manzanares, Spain [2]. The SUTPP prototype constructed in Manzanares worked for approximately 7 years and the results of preliminary experiments were presented by Haaf et al. [3, 4]. Regarding the literature review, SUTPPs have been investigated from various perspectives such as experimental methods [5], numerical and mathematical solutions [6, 7], and analytical studies [8, 9]. Comparison of all investigation methods of SUTPP shows that analytical or mathematical modeling is the suitable method to analyze the performance and power generation of SUTPP. One of the first analytical studies was carried out by Pasumarthi and Sherif [10]. They presented a mathematical model to investigate the performance of SUTPP. Pasumarthi and Sherif [11] compared the measured data of Manzanares SUTPP and obtained results of the mathematical model and illustrated the verification of the mathematical model. Koonsrisuk and Chitsomboon [12, 13] investigated the accuracy of five theoretical models of SUTPP performance and compared the obtained results by theoretical

*Corresponding author's email: msetare@jsu.ac.ir

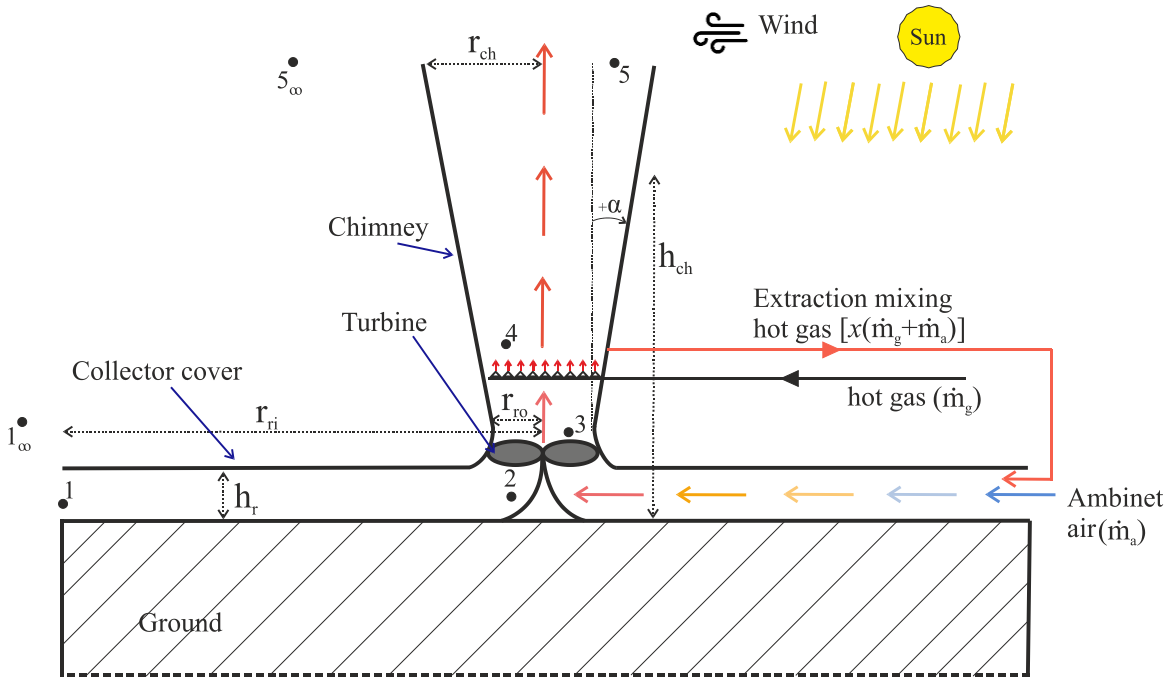

Fig. 1. Schematic drawing of a SUTPP with hot gas injection

models with those obtained by CFD simulation. Koonsrisuk [14] presented the one-dimensional mathematical model of a sloped solar chimney power plant and evaluated the accuracy of the model with the numerical simulation. Sangi et al. [15] studied numerically and mathematically the performance of SUTPP by Fluent software. They showed that the results of both numerical simulation and mathematical model have a reasonable agreement with the experimental data of Spanish SUTPP. In another research, the performance assessment of SUTPP regarding Iran's climate was mathematically carried out by Sangi [16]. He applied the energy balance approach and results demonstrated that the south and southwest of Iran have a considerable potential to generate electric power by means of SUTPP technology. Balijepalli et al. [17] studied mathematically the effect of various parameters such as the material of each component, geometric dimensions, and solar irradiation on the SUTPP performance. Ali et al. [18] used the simulink toolbox of Matlab software and presented a mathematical study on the performance of a SUTPP in any location worldwide with the case study in Kufa, Iraq. They reported that the annually power output in Kufa is obtained equal to 6122.3 kW. Singh et al. [19] presented a feasibility and mathematical study on the height of divergent chimney to generate the power output as equal as the power output of conventional SUTPP in Manzanares. They obtained that the height of the divergent chimney can be reduced up to 80% of the height of the conventional chimney at a specified power output.

To more detailed studies, some researchers investigated numerically the effect of influential parameters such as the radius and slope of the collector [20], the height and divergent angle of the chimney [21], collector configuration [22], the amount of incident solar energy [23] and using energy storage material [24] on the performance of SUTPP. The effect of chimney tilt angle, crosswind flow, and solar irradiation on the flow field and performance of a small-scale SUTPP was numerically studied by Rahimi Larki et al. [25]. They showed that crosswind flow has a negative effect on the performance of SUTPP and the adverse effect becomes severe at low wind velocity. Bagheri and Ghodsi Hassanabad [26] presented a new model of SUTPP in urban areas and evaluated numerically the performance of their proposed model. They found that vertical collector has a positive effect on the power output. Mandal et al. [27] investigated numerically the impact of geometric parameters such as the divergent angle of the chimney and the slope of the absorber on the energy efficiency of SUTPP. They reported that the power output is increased 80% for the SUTPP with the absorber angle of 0.6 degrees and chimney angle of 0.75 degrees as compared to classical Manzaranes SUTPP.

According to mentioned papers about theoretical and mathematical modeling and various methods for performance enhancement of SUTPP [28], some important issues can be pointed out as follows:

What are the governing equations for performance analysis of a SUTPP?

How can the performance of SUTPP enhanced?

What is the effect of geometric parameters and operation

Table 1. Geometric configuration of SUTPP [29].

Parameter	Value
Chimney height (h_{ch})	194.6 m
Collector height (h_r)	2.5 m
Collector radius (r_{ri})	122 m
Radius of Chimney base and collector outlet (r_{ro})	5.08 m
Radius of Chimney outlet (r_{co})	5.08 m

Table 2. Operating conditions and thermophysical and radiation characteristics [30, 31].

Parameter	Value
Ambient pressure at collector inlet ($p_{1\infty}$)	92.93 kPa
Ambient temperature at collector inlet ($T_{1\infty}$)	18.5 ^{o}C
Specific heat capacity of air and hot gas at constant pressure (c_p)	1004 J/kg. K
Collector cover transmittance (τ_c)	0.83
Collector floor (ground) absorptance (α_g)	0.9
Collector cover emittance (ε_c)	0.87
Collector floor (ground) emittance (ε_g)	0.9
Kinematic viscosity of air (υ)	1.63×10^{-5} m^2/s
Thermal conductivity of ground (k_g)	1.83 W/m. ^{o}C

conditions on the performance of SUTPP?

In order to answer the aforementioned questions, many papers have been reviewed and it is found that the SUTPP performance is enhanced remarkably with rising air temperature passing each part of the system. Indeed, air temperature rise causes to increase in the pressure potential, which is known as the driving force. In the present study, the effect of the injection of hot gas flow into the airflow passing the SUTPP and recirculation of a portion of mixed hot airflow as novel methods on the SUTPP performance are studied mathematically. The hot gas flow can be supplied by exhaust gases from equipment like a gas turbine, internal combustion engine, etc. A new one-dimensional mathematical model is developed to analyze the energy balance and momentum equations and power output. Besides, the effect of crosswind velocity on the power output is investigated.

2- Methodology

2- 1- Geometric description, reference conditions, and assumptions

Table 1 shows the dimensions of SUTPP, which are considered for mathematical modeling in the present study. The main dimensions are the same as the ones in the solar chimney power plant constructed in Manzanares, Spain in the early 1980s. The operating conditions as well as radiation characteristics of materials used for the collector section are written in Table 2. The principal assumptions in the present study are stated as follows:

The fluid flow field is considered axially passing each section of SUTPP.

The temperature distribution in each section is uniform.

The velocity distribution in each section is uniform.

The chimney's wall is insulated thermally.

The thermal properties of hot gas are approximated by the properties of air.

The fresh air and hot gas are modeled as an ideal gas.

Surface optical properties are considered constant.

2- 2- Theoretical modeling

The one-dimensional thermodynamic analysis is presented here to obtain the temperature, and pressure at each point shown in Fig. 1.

The mass flow rate at each point is an essential parameter to analyze the momentum and energy equations in the system. The total mass flow rate at positions labeled in Fig. 1 is obtained as follows:

$$\dot{m}_1 = \dot{m}_a + x\left(\dot{m}_a + \dot{m}_g\right) \tag{1}$$

$$\dot{m}_4 = \dot{m}_a + x\left(\dot{m}_a + \dot{m}_g\right) + \dot{m}_g = \left(1+x\right)\left(\dot{m}_a + \dot{m}_g\right) \tag{2}$$

$$\dot{m}_5 = \left(1+x\right)\left(\dot{m}_a + \dot{m}_g\right) - x\left(\dot{m}_a + \dot{m}_g\right) = \dot{m}_a + \dot{m}_g \tag{3}$$

where $\dot{m}_a$, $\dot{m}_g$ and x are the mass flow rate of air, the mass flow rate of hot gas, and extraction fraction, respectively.

2- 2- 1- Collector

The one-dimensional energy analysis for the collector regarding the positions numbered in Fig. 1 is given as follows [29]:

$$\dot{Q} + \dot{m}_1\left(h_1 + \frac{V_1^2}{2} + gZ_1\right) = \dot{m}_2\left(h_2 + \frac{V_2^2}{2} + gZ_2\right) \tag{4}$$

where $\dot{Q}$, h, V, g, and z are the heat added to the air from solar irradiance, enthalpy, velocity, gravitational acceleration, and height, respectively. The enthalpy, air velocity, density, and heat gain can be calculated as [14]:

$$\Delta h = c_p \Delta T \tag{5}$$

$$V = \frac{\dot{m}}{\rho A} \tag{6}$$

$$\rho = \frac{p}{RT} \tag{7}$$

$$\dot{Q} = q'' A_r \tag{8}$$

where c_p, T, $\dot{m}$, ρ and A and A_r are the specific heat coefficient at constant pressure, temperature, mass flow rate, density, and cross-sectional and collector roof area, respectively. By substituting Eqs. - into Eq. and assuming a horizontal collector, the temperature rise through the collector is obtained as follows [14]:

$$T_2 - T_1 = \frac{q'' A_r}{\dot{m}_2 c_p} + \frac{\dot{m}_1^2}{2\rho_1^2 c_p}\left(\frac{1}{A_1^2} - \frac{1}{A_2^2}\right) \tag{9}$$

The heat flux q'' is the solar energy added to the collector and is given by Eq. as follows [29]:

$$q'' = \alpha G - U_c\left(T_g - T_\infty\right) \tag{10}$$

where α_g, G, and U_c are the absorption coefficient of ground, the solar irradiance, and the heat transfer coefficient, respectively. For simplicity, T_g is assumed equal to $(T_1+T_2)/2$ and $T_\infty = T_1$. The heat transfer coefficient in Eq. is equal to the sum of the top and bottom loss coefficients of the collector. The top loss coefficient, U_t, is given by an empirical correlation presented by Kalogirou [32] as follows:

$$U_t = \frac{1}{\dfrac{N_g}{\dfrac{c}{T_{st}}\left(\dfrac{T_{av}-T_{amb}}{N_g+f}\right)^{\frac{1}{3}} + \dfrac{1}{h_w}} + \dfrac{\sigma\left(T_{av}^2 + T_{amb}^2\right)\left(T_{av}+T_{amb}\right)}{\dfrac{1}{\varepsilon_g + 0.05N_g\left(1-\varepsilon_g\right)} + \dfrac{2N_g + ff - 1}{\varepsilon_c} - N_g}} \tag{11}$$

where N_g is the number of glass covers which is equal to 1, σ is the Stefan-Boltzman constant, ε_g is the emissivity of the collector floor which is equal to 0.9, ε_c is the emissivity of collector glass which is equal to 0.87 and T_{av} is the arithmetic mean of air temperature at collector inlet and outlet. In addition, T_{st} and h_w are the stagnation temperatures at the collector inlet, and the heat transfer coefficient in windy

conditions as well as *c* and *ff* are constant. The following equations are applied to estimate the parameters in Eq.11 as follows [33]:

$$h_w = 5.67 + 3.87u \tag{12}$$

$$ff = \left(1 - 0.04h_w + 0.0005h_w^2\right)\left(1 + 0.091N_g\right) \tag{13}$$

$$c = 365.9\left(1 - 0.00883\theta + 0.0001298\theta^2\right) \tag{14}$$

where u and θ are the wind velocity and collector slope or collector tilt (degrees), respectively. The heat loss coefficient from the bottom is less as compared to the one from the top and is considered one-tenth of top heat loss [32].

The inlet temperature is calculated as follows:

$$T_1 = \frac{\dot{m}_a T_a + x\left(\dot{m}_a + \dot{m}_g\right)T_4}{\dot{m}_a + x\left(\dot{m}_a + \dot{m}_g\right)} \tag{15}$$

where T_a is the temperature of ambient air.

To determine pressure change across the collector, the continuity, momentum, energy, and state equations are used here. Eqs. - shows the differential form of governing equations for one-dimensional flow as follows [14]:

$$d\left(\rho VA\right) = 0 \;\rightarrow\; \frac{d\rho}{\rho} + \frac{dV}{V} + \frac{dA}{A} = 0 \tag{16}$$

$$dp = -\rho V dV - \rho g dz \tag{17}$$

$$c_p dT + V dV + g dz = dq \tag{18}$$

$$\frac{dp}{p} - \frac{d\rho}{\rho} - \frac{dT}{T} = 0 \tag{19}$$

where q is the absorbed heat by airflow inside the collector per mass flow rate. By dividing the momentum equation shown in Eq. by p and replacing ρ with the ideal gas law as well as using the Mach number, the momentum equation yields as follows [14]:

$$\frac{dp}{p} = -\gamma M^2 \frac{dV}{V} - g\frac{dz}{RT} \tag{20}$$

where M and γ are the Mach number and heat capacity ratio, respectively. Mach number is defined as the ratio of flow velocity to local sound speed $C = \sqrt{\gamma RT}$.

By substituting Mach number into Eq. and using the thermodynamic relation $R=c_p-c_v$, the rearranged energy equation is written as follows [14]:

$$\frac{dT}{T} = \frac{dq}{c_p T} - \left(\gamma - 1\right)M^2 \frac{dV}{V} - \frac{gdz}{c_p T} \tag{21}$$

Next, by substituting Eq. and Eq. into the equation of state illustrated in Eq. , the density difference is obtained. Then, substituting the derived density difference into the continuity equation, Eq. , the velocity difference for low Mach number regime is written as follows [14]:

$$\frac{dV}{V} = \left(\frac{gdz}{\gamma RT} + \frac{dq}{c_p T} - \frac{dA}{A}\right) \tag{22}$$

Combining Eq. and Eq. , the pressure difference with an assumption of $M<<1$ is derived as [14]:

$$dp = -\rho g dz + \rho V^2 \left(\frac{dA}{A} - \frac{dq}{c_p T}\right) \tag{23}$$

Let's consider $dq = q'' dA_s / \dot{m}$ and $\dot{m} = \rho VA$, and then substitute them into Eq. , the simplified pressure difference is obtained as follows [14]:

$$dp = -\rho g dz + \frac{\dot{m}^2}{\rho}\frac{dA}{A^3} - \frac{q''\dot{m}}{\rho c_p T}\frac{dA_s}{A^2} \tag{24}$$

where dA and dA_s are infinitesimal elements of cross-sectional area and infinitesimal elements of collector roof area, respectively. By substituting $dA_s=2\pi r dr$ and $A=2\pi r h_r$, the pressure difference across the collector is obtained as follows [34]:

$$p_2 - p_1 = \rho g\left(z_1 - z_2\right) - \frac{\dot{m}^2}{2\rho}\left[\frac{1}{A_2^2} - \frac{1}{A_1^2}\right] - \frac{q''\dot{m}}{2\rho c_p T\,\pi h_c^2}\ln\frac{r_2}{r_1} \tag{25}$$

where all thermophysical properties are estimated at the temperature of the collector inlet.

2- 2- 2- Turbine

By combining the first and second laws of thermodynamics and neglecting potential and kinematic energy changes, the power output of the turbine for an isentropic process is derived as follows [14]:

$$P_t = -\dot{m}_2 \int_2^3 \upsilon dp = -\frac{\dot{m}_2}{\rho_{ave}} \Delta p_t \tag{26}$$

where P_t is the power output, and ρ_{ave} is the average density of air passing through the turbine and Δp_t is the pressure drop across the turbine, which is equal to p_3-p_2. The turbine pressure drop is obtained according to the draught equation which is fully explained in the following sections.

The air temperature after the turbine section is also calculated by energy balance as follows [31]:

$$T_3 = T_2 + \frac{P_t}{\dot{m} c_p} \tag{27}$$

2- 2- 3- Chimney

The temperature of flow at the chimney base is considered to be equal to the temperature of the mixed flow of hot gasses and airflow passing the turbine. The temperature of the mixed flow is obtained as follows:

$$T_4 = \frac{\left[\dot{m}_a + x\left(\dot{m}_a + \dot{m}_g\right)\right] T_3 + \dot{m}_g T_g}{\left(1+x\right)\left(\dot{m}_a + \dot{m}_g\right)} \tag{28}$$

where T_3 and T_4 are the air temperature after the turbine section and the temperature of the mixed flow of hot gasses and airflow passed the turbine, respectively. It is necessary to mention that the temperatures of airflow passing the turbine and injected hot gas are different. Therefore, complete mixing of airflow passing the turbine and injected hot gas is done in a place above the injection point. In the present study, point 4 is the place where the airflow and injected hot gas are well mixed. In addition, in the numerical solution, it is assumed that the mixing length, the distance between the injection point and point 4, is infinitesimal and the injection point and point 4 are placed at the same elevation.

The energy equation for the chimney is as same as one for the collector except the solar irradiance on the chimney surface is equal to zero, i.e. the chimney is covered completely by thermal insulation. Therefore, the temperature at the chimney outlet is given by Eq. as follows [31]:

$$T_5 - T_4 = -\frac{g}{c_p} h_{ch} + \frac{\dot{m}_5^2}{2\rho_4^2 c_p}\left(\frac{1}{A_4^2} - \frac{1}{A_5^2}\right) \tag{29}$$

The chimney is like a circular cylinder with a constant cross-sectional area, thus the second term on the RHS of Eq. is equal to zero. It is noteworthy that the temperature at each position of the chimney can be estimated by the dry adiabatic lapse rate (DALR) relation as follows [35]:

$$T = T_4 - \frac{g}{c_p} z \tag{30}$$

where z is the vertical coordinate.

For the frictionless flow inside the chimney and supposing the insignificant impact of velocity changes on the flow field because of small changes in the cross-sectional area of the chimney, the momentum equation for the chimney is written as follows [14]:

$$dp = -\rho g dz \tag{31}$$

By substituting ρ with the equation state of an ideal gas and using the DALR equation written in Eq. then integrating it between the inlet and outlet of the chimney, the pressure at the chimney base yields as follows [14]:

$$p_4 = p_5 \left(1 - \frac{g h_{ch}}{c_p T_4}\right)^{\frac{-\gamma}{\gamma-1}} \tag{32}$$

where γ is the specific heat ratio of air. The velocity of atmospheric air at the same height of the chimney outlet is rather low, therefore the air pressure at the chimney outlet and atmospheric pressure at the same height are considered to be equal, i.e. $p_5 = p_{5\infty}$.

2- 2- 4- Driving Force

The driving force or driving pressure potential which is generated by density variations of the air associated with temperature changes, is basically the pressure difference between the cold air column outside the tower and the hot air column inside the tower. Eq. which is called the draught equation, shows the driving pressure potential equation as follows [30]:

$$\Delta p_{pp} = \left(p_1 - p_{5\infty}\right) - \left(p_4 - p_5\right) \tag{33}$$

where Δp_{pp} is the driving pressure potential and 1, 4, 5, and 5∞ subscripts show different positions of the SUTPP system regarding Fig. 1. To consider the impact of ambient wind,

Table 3. The value of loss coefficient [30, 31, 37].

Parameter	K
$\Delta p_{col,i}$	1
$\Delta p_{t,i}$,	0.25
$\Delta p_{ch,o}$	$\left(\rho_{5\infty}V_{5\infty}^2/\rho_5 V_5^2\right)\left(c_{po}-1\right)+1$
Δp_{dyn}	1
$\Delta p_{f,col}$	fL/d
$\Delta p_{f,ch}$	fL/d

Zhou et al. [36] proposed to calculate the driving pressure potential as follows:

$$\Delta p_{pp} = p_{1\infty}\left(1-\left(\frac{1-\frac{gh_{ch}}{c_pT_{1\infty}}}{1-\frac{gh_{ch}}{c_pT_4}}\right)^{\frac{\gamma}{\gamma-1}}\right) + \frac{\rho_{5\infty}\left(c_{po}-1\right)u^2}{2}\left[1-\left(1-\frac{gh_{ch}}{c_pT_4}\right)^{\frac{-\gamma}{\gamma-1}}\right] \tag{34}$$

where c_{po} and u are pressure coefficient and ambient wind velocity, respectively. The pressure coefficient is calculated by an empirical formula as [36]:

$$c_{po} = -0.405+1.07\left(\frac{u}{V_5}\right)^{-1} +1.8\left[\left(\frac{u}{V_5}\right)\left(\frac{A_5}{A_t}\right)^{1.65}\right]^{-2}\log_{10}\left[\left(\frac{u}{2.7V_5}\right)\left(\frac{A_5}{A_t}\right)^{1.65}\right] +\left[-1.04+1.0702\left(\frac{A_5}{A_t}\right)-0.662\left(\frac{A_5}{A_t}\right)^2\right]\left(\frac{u}{V_5}\right)^{-0.7} \tag{35}$$

where A_t is the throat cross-sectional area of the chimney, A_5 is the cross-sectional area at the chimney outlet and V_5 is the flow velocity at the chimney outlet. It is clear that A_t=A_4 regarding the schematic view of SUTPP shown in Fig. 1.

The turbine pressure drop is calculated by the draught equation which is equal to the subtraction of all pressure losses through the system from driving pressure potential as follows [30]:

$$\Delta p_t = \Delta p_{pp} - (\Delta p_{col,i} + \Delta p_{t,i} + \Delta p_{ch,o} + \Delta p_{f,col} + \Delta p_{f,ch} + \Delta p_{dyn}) \tag{36}$$

where $\Delta p_{col,i}$, $\Delta p_{t,i}$, $\Delta p_{ch,o}$, $\Delta p_{f,col}$, $\Delta p_{f,ch,}$ and Δp_{dyn} are the pressure loss at collector entrance, the pressure loss at turbine inlet, the pressure loss at chimney exit, the pressure loss due to viscous effects in the collector, the pressure loss due to viscous effects in the chimney and dynamic pressure loss of outlet flow from the chimney, respectively. The ratio of turbine pressure drop to driving pressure potential (*PR*) is an appropriate criterion to investigate the performance and find the optimal operating condition of SUTPP, which is defined as follows [29]:

$$PR = \frac{\Delta p_t}{\Delta p_{pp}} \tag{37}$$

2- 2- 5- Calculation of pressure drops

Eq. is used to compute pressure drops at each part of the system as follows [30]:

$$\Delta p = K\frac{\rho V^2}{2} \tag{38}$$

where K is a dimensionless parameter which is named loss coefficient. The value of K for all pressure drops through the system is given in Table 3.

The friction factor is required to calculate the frictional pressure drops in the collector and chimney. The relation proposed by Haaland [38] is used here as follows:

$$f=\left\{-1.8\log\left[\left(\frac{6.9}{\mathrm{Re}_d}\right)+\left(\frac{\varepsilon/d}{3.75}\right)^{1.11}\right]\right\}^{-2} \quad (39)$$

where ε is the roughness height and is equal to 0 and 0.002 mm for the collector roof and chimney wall, respectively [30].

2- 3- Solution algorithm

With the detailed investigation of the aforementioned formulation, it is found that the value of air mass flow rate should be known in order to obtain the power output, turbine pressure drop, etc. Therefore, for an assumed $\dot{m}_a$ at a specified $\dot{m}_g$ and solar irradiance as well as extraction fraction, both temperature difference of air inside the collector and the air temperature at the collector outlet are calculated by Eq. . Because the heat flux shown in Eq. and collector top loss coefficient depend on the air temperature at the collector outlet, an iterative method must be applied to obtain the air temperature at collector outlet (T_2). In addition, because the fresh air and a mixture of air and hot exhaust gas extracted after the turbine are mixed at the collector inlet, the temperature of mixed flow at this section as shown in Eq. should be determined by a trial and error method as well. After obtaining the temperature at the collector outlet, the pressure difference of air inside the collector can be calculated by Eq. . The temperature of air after passing the turbine, T_3, is also unknown and is guessed to calculate the temperature of the mixture of hot gas injection and the airflow passing the turbine, and the temperature of flow at the collector inlet. Next, all pressure drops through the system are calculated by Eq. , and the driving pressure potential is obtained by Eq. . The turbine pressure drop is computed with regard to the pressure balance formula in Eq. , and consequently, the power output is calculated by Eq. . To verify the guessed temperature T_3, the air temperature after the turbine obtained by using the first law of thermodynamics in Eq. is compared with the guessed one. It is clear that an iterative scheme must be applied to calculate T_3 like the procedure for T_2. Here, the convergence criterion is set equal to 10^{-4}. Now, if the power output is positive, the SUTPP has meaningful performance and the solution procedure is repeated for a new $\dot{m}_a$. The flowchart of the solution procedure is illustrated in Fig. 2.

3- Results and discussions

A new computational code in MATLAB is developed to simulate the impact of different parameters and environmental conditions on the SUTPP performance. The dimensions of the SUTPP system are written in Table 1 and the investigation of SUTPP performance under hot flue gas injection after the turbine section as well as extracting a portion of mixed air and injecting it at the collector inlet is carried out.

3- 1- Validation model results against experimental data

The verification of the presented computational code is investigated by comparing the model results with the reference data presented by Schlaich et al. [39] on Manzanares SUTPP. Here, all dimensions and other conditions similar to those of SUTPP in Manzanares are considered as input data to computational code, and the comparison between model results and experimental data is investigated.

Fig. 3 represents the maximum power output at a specified solar irradiance as a function of updraft velocity by experimental data reported in Ref. [40] and the present theoretical method. Comparison between the result of the present theoretical model and measured data illustrates that results obtained by the present method are in agreement with the experimental data and consequently, the accuracy and reliability of the present method are verified. For further investigation, the temperature rising of air inside the collector obtained by the present mathematical model and experimental data by Haaf [3] from SUTPP in Manzanares is plotted in Fig. 4. It can be seen that the results of the present theoretical model are in good consistent with the experimental data. The maximum error of 15% at solar irradiance of 750 W/m^2 and the error of less than 10% at other points verify that reliable and acceptable results are obtained by the present theoretical model.

3- 2- Model results

The influence of different parameters including extraction fraction, hot gas mass flow rate, and wind velocity on the SUTPP performance is studied in the present section. First, the solar irradiance, wind velocity, and hot gas flow rate are considered equal to 850 W/m^2, 10 m/s, and 10 kg/s, respectively. Fig. 5 shows the variations of driving pressure potential, i.e., driving force, as a function of air mass flow rate at the collector inlet for different extraction fractions. Results demonstrate that the driving pressure potential decreases as the mass flow rate increases, which is due to increasing the amount of pressure drops through the system. In addition, it is found that at a specified $\dot{m}_1$, the driving pressure potential increases slightly for a higher extraction fraction.

The turbine power output for different extraction fractions is shown in Fig. 6. Results show that at a specified $\dot{m}_1$, the power output increases with increasing extraction fraction. The reason can be explained that with the injection of hot gas at the chimney base, the temperature of airflow passing the chimney is increased due to mixing with hot gas. Consequently, the driving pressure potential becomes higher. Besides, the extraction of a portion of the mixed flow and reinjected it into the collector inlet causes the temperature of airflow at the turbine inlet, i.e. collector outlet, to increase, and the power output increases as well. Besides, for a specified x, the turbine power output increases from zero to a maximum value with increasing $\dot{m}_1$. The best operation condition of SUTPP is where the maximum power output occurs. At this point, the mass flow rate and flow velocity and momentum rate for x of 0% are equal to 540 kg/s, 6.5 m/s, and 3545 kg.m/s^2, for x of 10% are equal to 616 kg/s, 7.5 m/s and 4613.7 kg.m/s^2, for x of 20% are equal to 660 kg/s, 8.05 m/s and 5309.7 kg.m/s^2, for x of 30% are equal to 715 kg/s, 8.73 m/s and 6243.1 kg.m/s^2, and for x of 40% are equal to 756 kg/s, 9.25 m/s and 6998.1

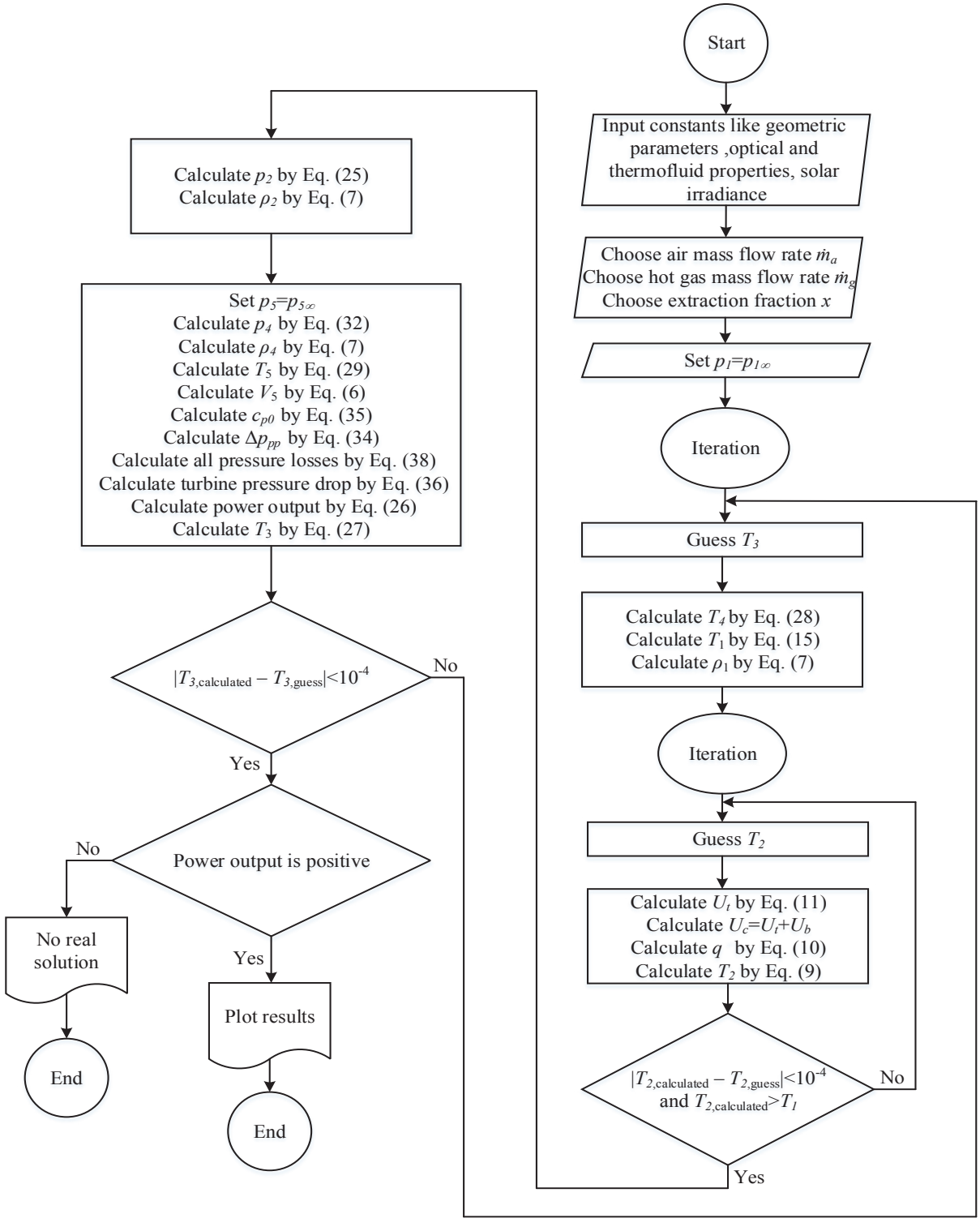

Fig. 2. Solution algorithm flowchart.

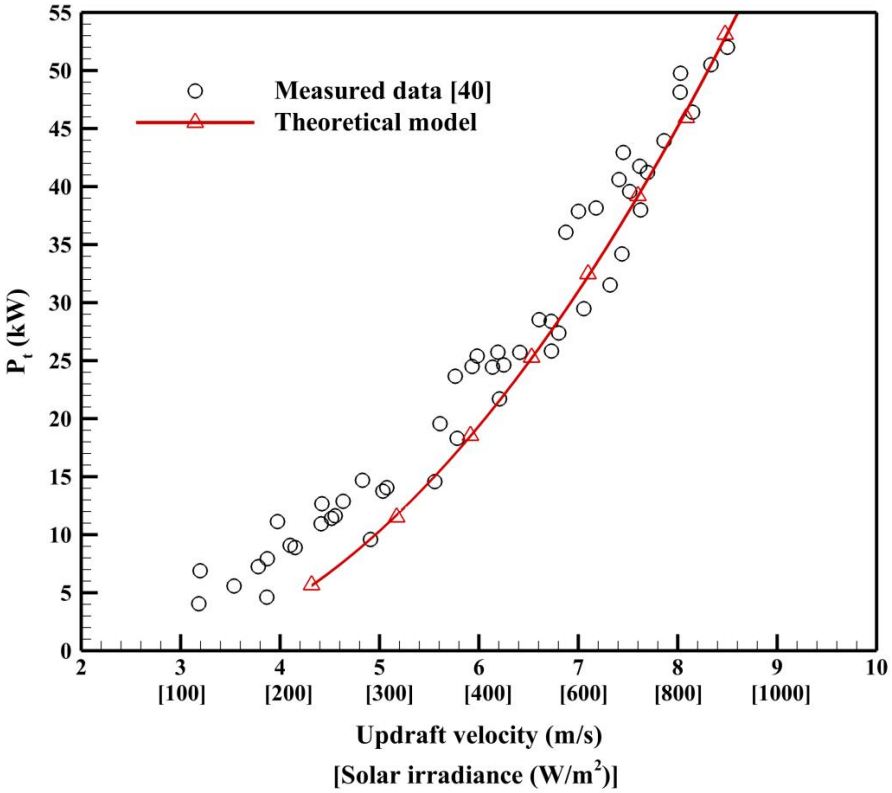

Fig. 3. Comparison between measured data and results of the theoretical model.

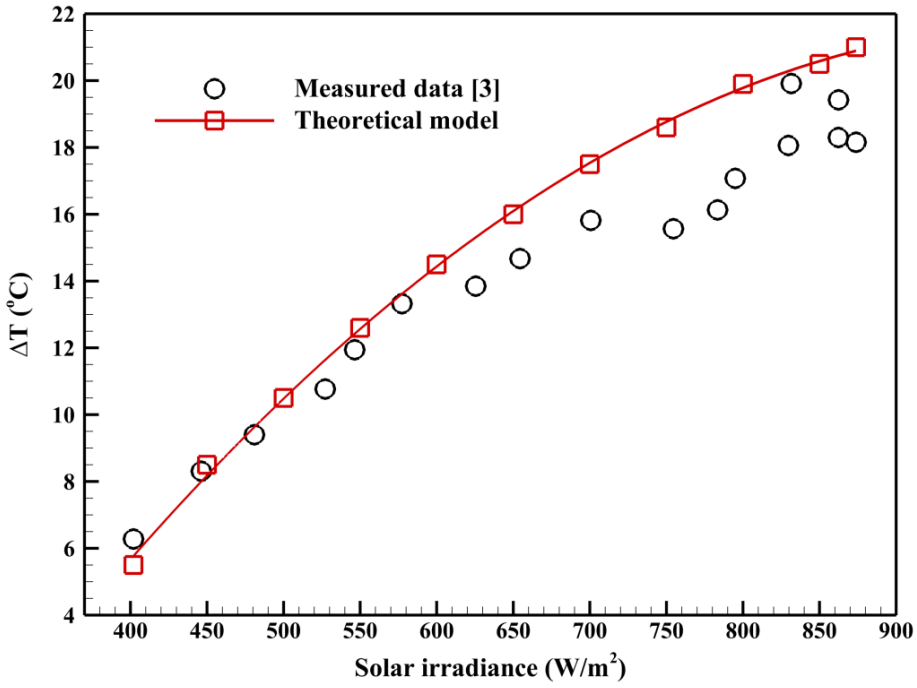

Fig. 4. Temperature rising of air inside the collector by the present theoretical method and experimental data by Haaf [3].

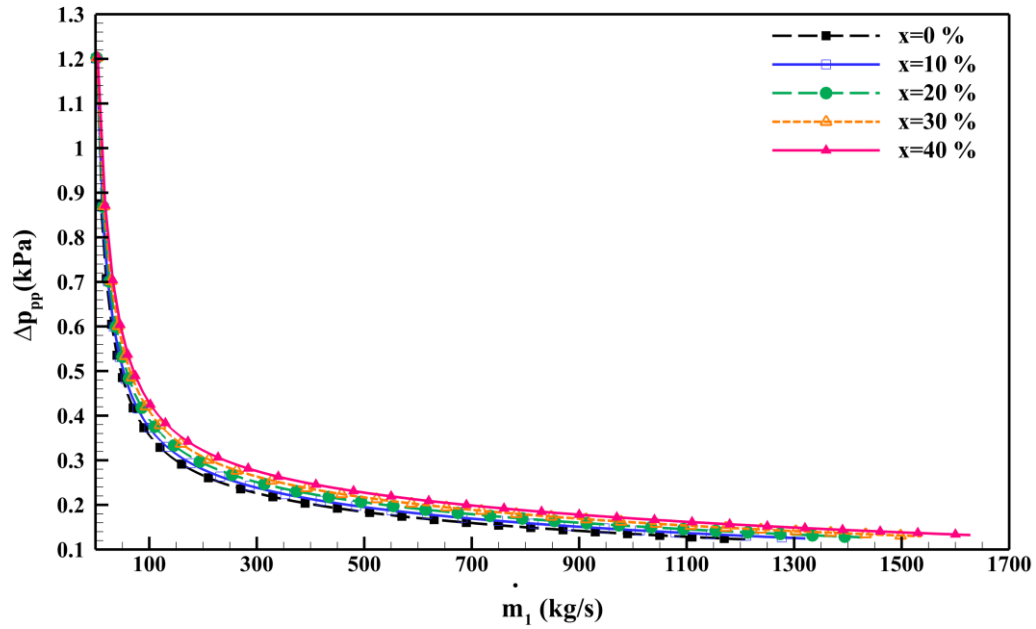

Fig. 5. Driving force as a function of mass flow rate at collector inlet at G=850 W/m2 and u=10 m/s for different extraction fractions.

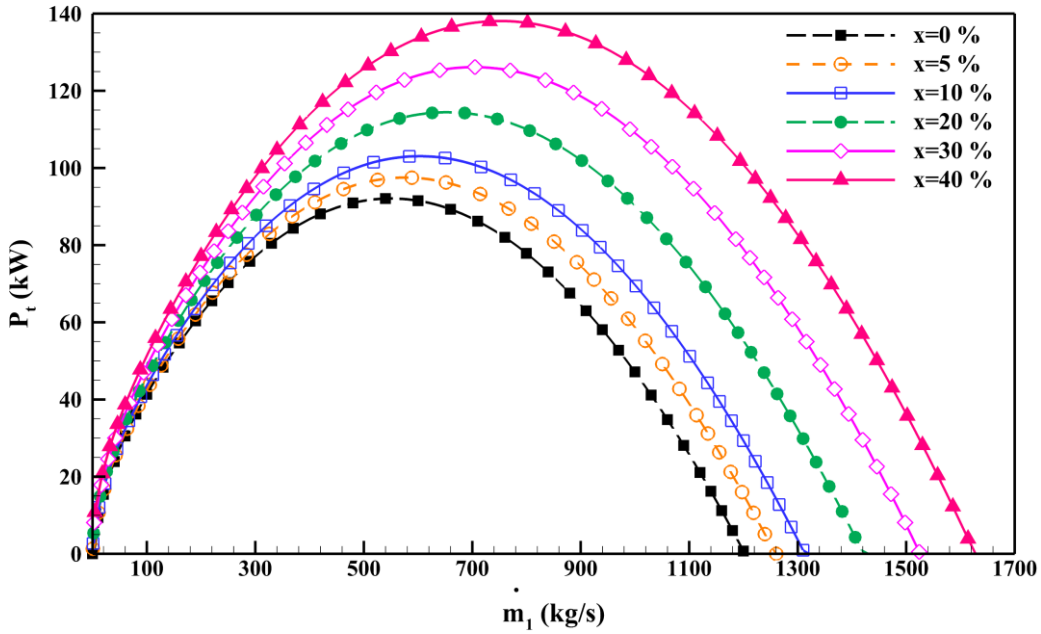

Fig. 6. Turbine power output as a function of mass flow rate at collector inlet at G=850 W/m2 and u=10 m/s for different extraction fractions.

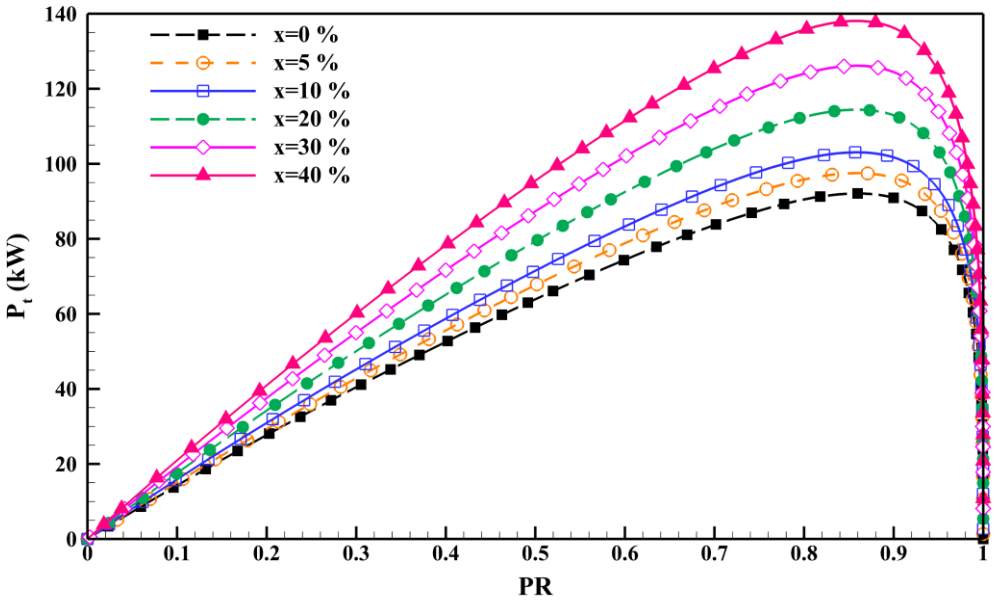

Fig. 7. Turbine power output as a function of PR parameter at G=850 W/m2 and u=10 m/s for different extraction fractions.

kg.m/s^2, respectively. It is noted that the rate of momentums is rather high which makes extracted mixed flow move easily toward the collector inlet. Beyond the optimal condition, P_t declines to zero with increasing $\dot{m}_1$. It is noteworthy that the higher $\dot{m}_1$, the higher pressure losses through the system, and it can be concluded that the negative impact of pressure losses becomes higher than the positive effect of driving pressure potential on turbine pressure drop regarding Eq. for $\dot{m}_1$ larger than $\dot{m}_1$ associated with maximum P_t. The second time in which P_t becomes zero is when the driving pressure potential is exactly equal to the sum of pressure losses and consequently, Δp_t becomes zero.

In most numerical and analytical previous research, the *PR* and Δp_t are preset, whereas these parameters are calculated in the present study. The relation between P_t and *PR* is shown in Fig. 7. At *PR*=1, the P_t is equal to zero, even though Δp_t is equal to Δp_{pp}. Actually, there is no airflow inside the collector, and consequently, the turbine power output becomes zero. The P_t is also equal to zero at *PR*=0. At this point, the Δp_t is equal to zero too, which means that the driving pressure potential is dissipated totally by pressure losses through various parts of the system. Results in Fig. 7 show that at each *x*, the P_t achieves the maximum value which is the optimal operating condition of SUTPP.

To study the effect of the mass flow rate of hot gas injection, the power output as a function of fresh air mass flow rate for different values of extraction fraction and hot gas flow rate is plotted in Fig. 8. Results indicate that P_t increases with increasing $\dot{m}_g$ for all extraction fractions at a specified $\dot{m}_a$. It can be clarified that the increase in $\dot{m}_g$ leads to an increase in the total mass flow rate of air including hot gas and fresh air and consequently, the power output becomes higher. In addition, a more detailed look at Fig. 8 shows that at a specified $\dot{m}_g$, the higher the maximum P_t, the higher *x*. For example, at $\dot{m}_g$ of 30 kg/s, the maximum P_t for *x* of 5%, 10%, 20%, and 30% is equal to 134.7 kW, 142.07 kW, 157.1 kW, and 172.6 kW, respectively. Furthermore, the locus of maximum power output at each $\dot{m}_g$ is represented by a dashed line in Fig. 8.

The extraction fraction is an effective parameter and its value has a remarkable effect on the performance of SUTPP. To show the influence of complete extraction of hot gas and reinject it into the collector inlet, the power output at *x* of 1 as a function of *PR* for different hot gas mass flow rates is illustrated in Fig. 9. It is evident that the turbine power output increases as the extraction fraction increases. Because the temperature of mixed hot gas and fresh air at the collector inlet as well as the temperature of mixed flow at the collector outlet increases with increasing the extraction fraction, it can be expected that the turbine power output becomes higher as the extraction fraction increases. However it is noteworthy that the entire injection of hot gas at the collector inlet is facing an operational problem. Actually, the collector is like a cylinder with a large diameter and short height. To take airflow with a uniform temperature at the collector inlet, the hot gas must be injected uniformly at the lateral surface of the cylinder and this issue is a very important operational restriction. In the present study, we propose to inject hot gas at the chimney base and reinject a portion of hot mixed flow into the collector inlet to solve this restriction. The cross-

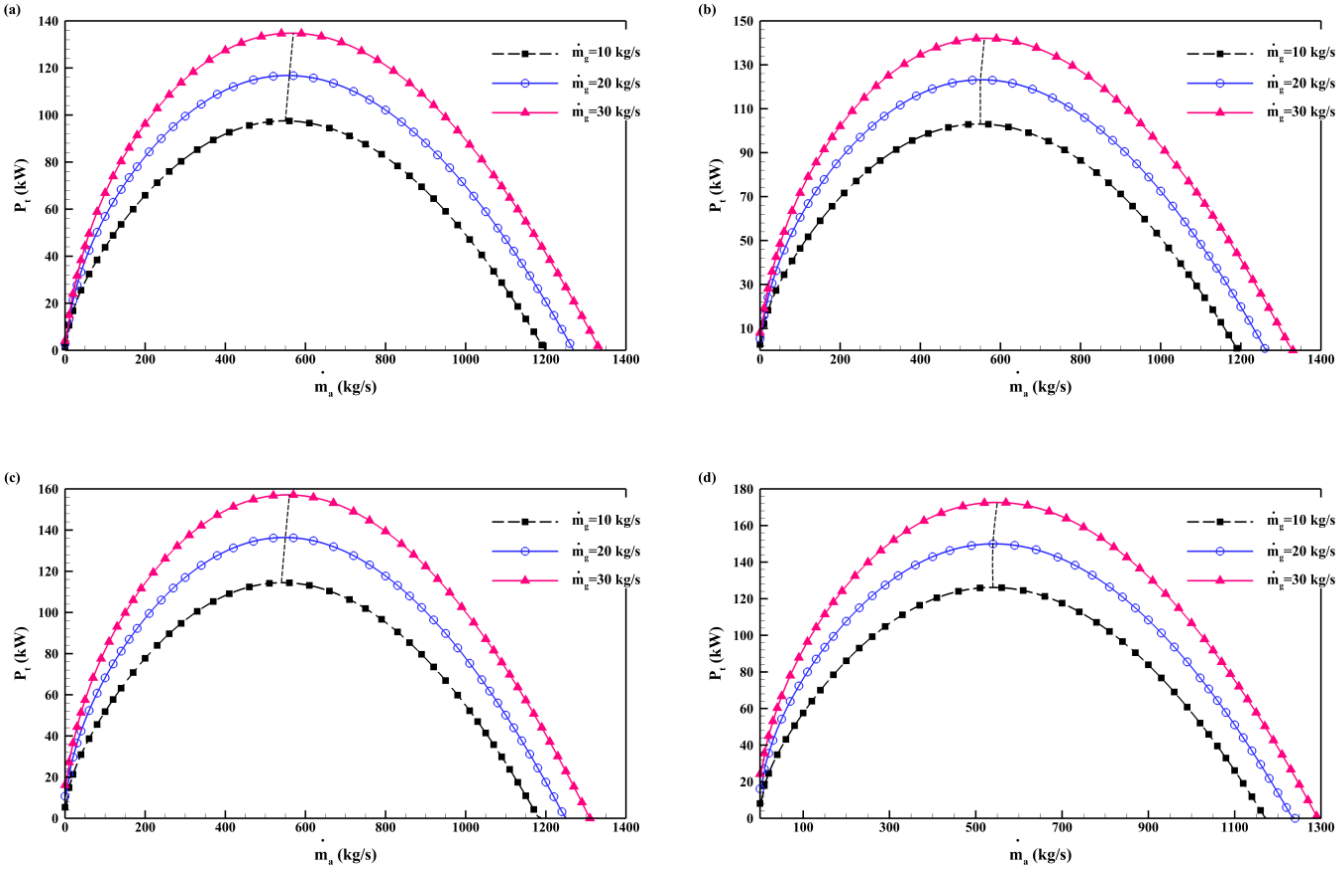

Fig. 8. Turbine power output as a function of air mass flow rate at G=850 W/m² and u=10 m/s for different mass flow rates of hot gas (a) x=5%, (b) x=10%, (c) x=20%, (d) x=30%.

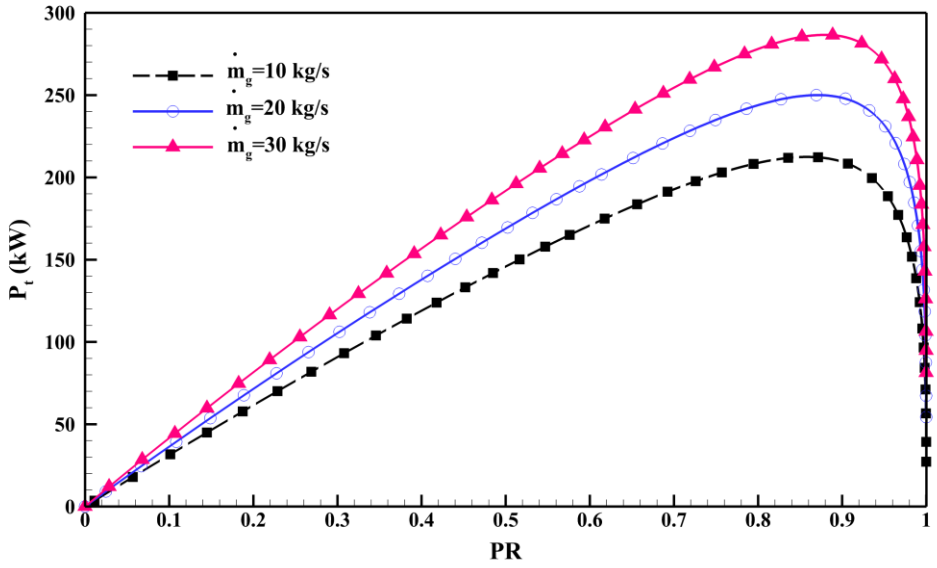

Fig. 9. The turbine power output as a function of PR for extraction fraction of 1 and u of 10 m/s.

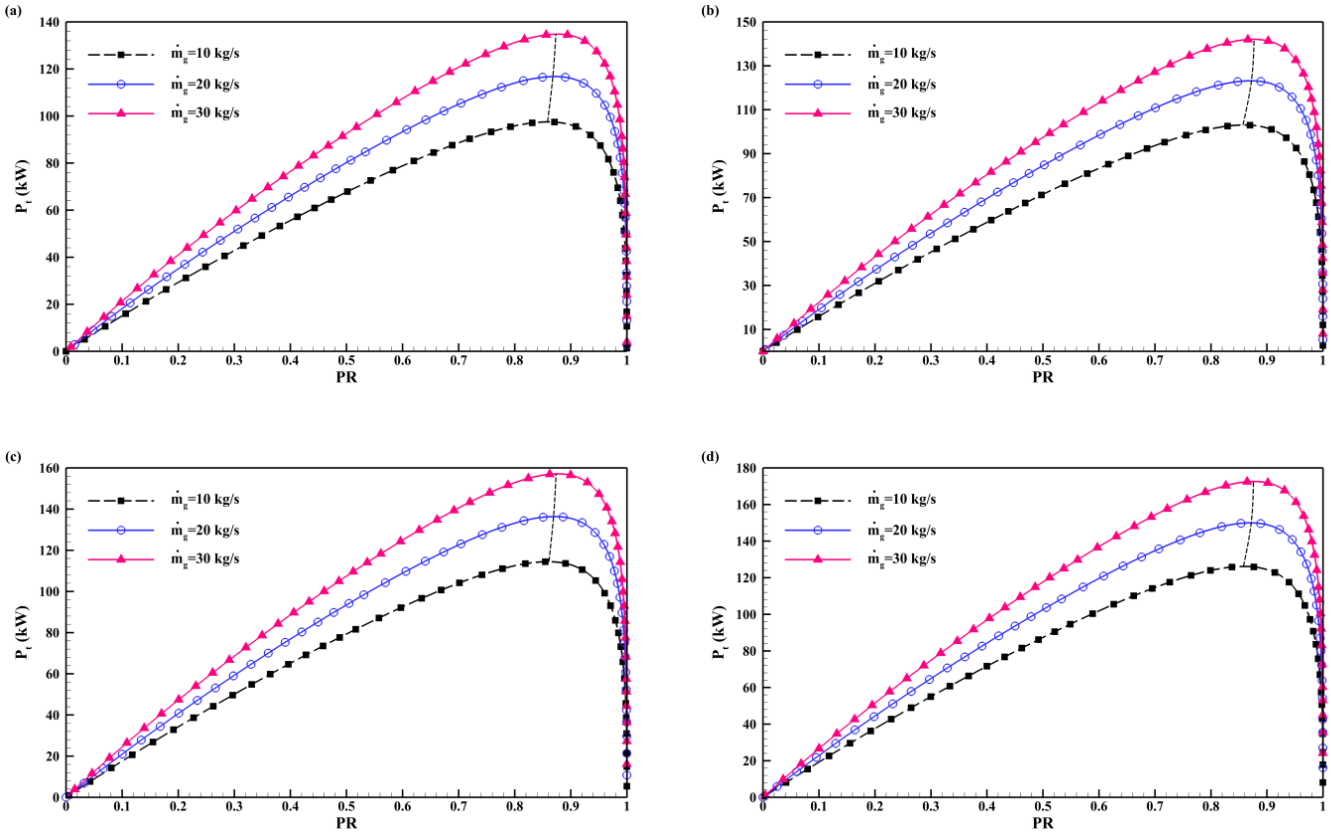

Fig. 10. Turbine power output as a function of PR parameter at G=850 W/m² and u=10 m/s for different mass flow rates of hot gas (a) x=5%, (b) x=10%, (c) x=20%, (d) x=30%.

sectional surface of the chimney is much lower than the lateral surface of the collector and the airflow and hot gas are well mixed at a short distance from the injection point.

To more study and reveal the effect of $\dot{m}_g$ on the SUTPP performance, the power output as a function of *PR* for various *x* is plotted in Fig. 10. Results show that the P_t increases with increasing $\dot{m}_g$ at a constant *PR*. Besides, the maximum power outputs for various $\dot{m}_g$ at each *x* are designated by a dashed line. By comparing the results in Fig. 10a-b, it is recommended to choose *PR* in a range from 0.83 to 0.87 to attain the optimal performance of SUTPP.

To investigate the impact of extraction fraction at optimum performance conditions of SUTPP, the maximum power output as a function of extraction fraction at each hot gas mass flow rate is plotted in Fig. 11. Results indicate that the maximum power output increases as the extraction fraction increases. As explained before, the higher the extraction fraction, the higher the temperature of mixed flow at the collector entrance, and consequently, the higher the amount of power output obtained. In addition, results show that the power output is higher for a higher hot gas mass flow rate at a specified extraction fraction. For a specified *x*, the higher amount of hot mixed air flow is extracted as the $\dot{m}_g$ increases, consequently, the higher amount of mixed air flow is injected at the collector inlet and it is expected that the temperature of mixed air at the collector inlet becomes higher. As a result, the maximum power output becomes higher.

To investigate the influence of wind velocity on the SUTPP performance, the power output at different wind velocities and extraction fractions is illustrated in Fig. 12. It can be concluded from the results that wind velocity has a beneficial impact on the power output, i.e., the higher power output is generated by higher wind velocity. In addition, the positive influence of wind velocity on the power output becomes severely larger from *u* of 20 m/s to 30 m/s. Comparing the results indicates that wind velocity has a more positive effect on power output at lower extraction fractions. For example, at *x*=5%, the P_t at *u* of 30 m/s and 20 m/s as compared to one at *u* of 10 m/s have enhanced by 386.1% and 113.5%, respectively. While at *x*=20%, the power output has augmented by 374.4% and 110.4% for *u* of 30 m/s and 20 m/s, respectively, as compared to one at *u* of 10 m/s.

4- Conclusion

In this research, a theoretical model was presented to investigate the effect of hot gas injection on the performance enhancement of SUTPP. An axisymmetric configuration was considered and it was assumed that the airflow entered axially

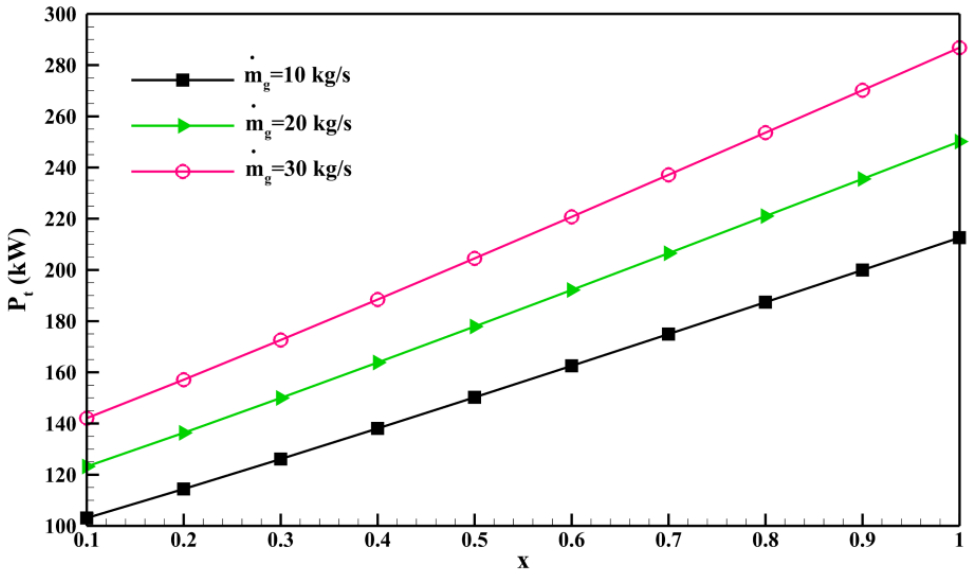

Fig. 11. Maximum power output as a function of extraction fraction at and u of 10 m/s.

at the collector inlet and passed through the collector, turbine, and chimney along the axial coordinate of each component. To calculate power output, the pressure drop across the turbine was obtained by the draught equation in which driving pressure potential in the presence of wind was computed by DALR relation and experimental correlation of pressure coefficient. Then, by using the obtained pressure drop, the power output was calculated with a trial and error method. To validate the proposed mathematical method, the geometric and operating conditions considered similar to ones in the Manzanares SUTPP, were applied in the present mathematical code and the obtained results were compared with the measured data. According to a slight difference between mathematical results and measured data of the Spanish SUTPP prototype, the validation of the present method was verified. Regarding the main purpose of the present paper which is the study on the influence of hot gas injection on the SUTPP performance, the effect of various mass flow rates of hot gas and extraction fraction of mixed airflow from the chimney and re-entered it into the collector was investigated. Results showed that at a specified air mass flow rate inside the collector, the driving pressure potential and pressure drop across the turbine were increased with increasing extraction fraction (x). Therefore, it can be expected that the power output becomes higher with increasing x. With the evaluation of power output at various x as a function of the mass flow rate entered at the collector inlet, the optimum SUTPP performance was declared. In addition, the power output at different mass flow rates was studied and results demonstrated that the higher the mass flow rates of hot gas, the higher the power output. The ratio of pressure drop across the turbine to total driving pressure potential (PR) was introduced as an assessment criterion and results showed that PR should be taken in the range from 0.83 to 0.87 to achieve the best performance. The effect of wind velocity was also investigated and the obtained results illustrated that the higher the wind velocity, the greater the positive impact of wind on the power output. For example, at $\dot{m}_g$= 10 kg/s and x=5%, the maximum power output has increased by 386.1% and 113.5% at wind velocity of 30 m/s and 20 m/s as compared to the maximum power output at wind velocity of 10 m/s, respectively.

5- Acknowledgments

This work has been financially supported by the research of Jundi-Shapur Research Institute. The grant number and grant code were 1753/17 and 1400_1_100_04, respectively.

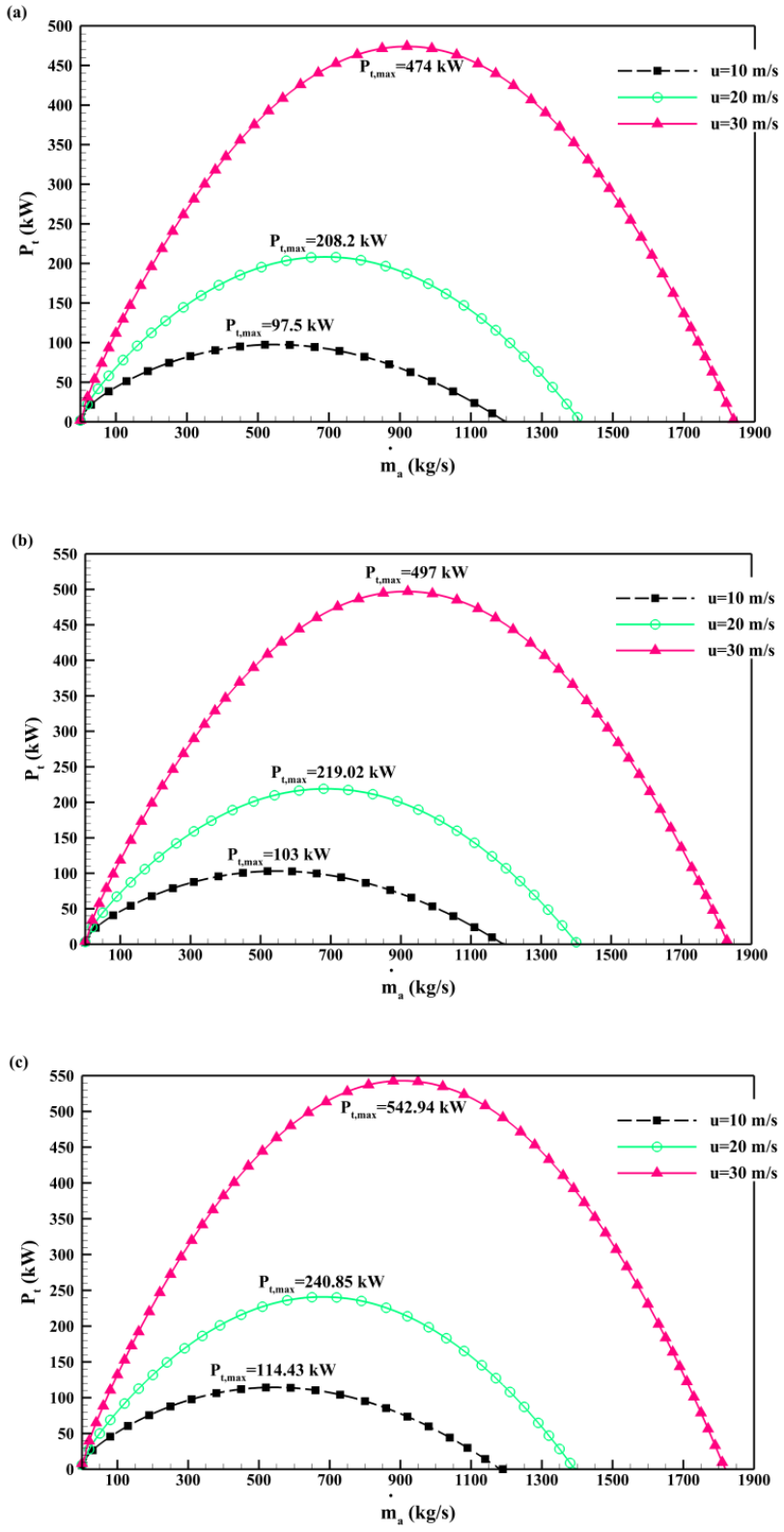

Fig. 12. The effect of wind velocity on turbine power output at ṁg=10 kg/s and different extraction fractions (a) x=5%, (b) x=10%, (c) x=20%.

Nomenclature

A	Area, m^2
Ar	Collector roof area, m^2
C	Sound speed, m/s
c	Constant
c_p	Specific heat capacity at constant pressure, J/kg. K
c_v	Specific heat capacity at constant volume, J/kg. K
c_{po}	Pressure coefficient
d	Diameter, m
f	Darcy friction factor
ff	Constant
G	Solar irradiance, W/m^2
g	Gravitational acceleration, m/s^2
h	Enthalpy, kJ/kg
h_c	Average collector height, m
h_{ch}	Chimney height, m
h_w	Heat transfer coefficient in the presence of wind, W/m^2. K
K	Coefficient
k	Thermal conductivity, W/m.°C
M	Mach number
$\dot{m}$	Mas flow rate, kg/s
N_g	The number of covers
p	Pressure, Pa
$\dot{Q}$	Added thermal power, W
q''	Heat flux, W/m^2
R	Gas constant, J/kg. K
Re	Reynolds number
r	Radius, m
T	Temperature, °C
U_c	Heat transfer coefficient, W/m^2. K
U_t	Top loss coefficient, W/m^2. K
u	Wind velocity, m/s
PR	The ratio of pressure drop across the turbine to driving pressure potential
p_t	Power output, kW
V	Velocity, m/s
x	Extraction fraction
Z	Height, m
z	Axial coordinate, m

Subscripts

1	Collector inlet
2	Collector outlet
3	After the turbine
4	After injection
5	Chimney outlet
∞	Far field
a	Fresh air
amb	Ambient
av	Average
ch,o	Position at chimney outlet
col,i	Position at collector inlet
dyn	dynamic
f,ch	Frictional over the chimney
$f,coll$	Frictional over the collector
g	Hot gas or ground
pp	Driving pressure potential
t	Turbine or throat
t,i	Position at the turbine inlet

Greek letters

α	Absorptivity
γ	Heat capacity ratio
Δ	Difference
ε	Wall roughness or Emissivity
υ	Specific volume, m^3/kg
ρ	Density, kg/m^3
τ	Transmissivity

References

[1] I. Cabanyes, Las Chimeneassolares (Solar Chimneys), La Ernergiaeléctr., (1903).

[2] L. Zuo, L. Ding, Y. Yuan, Z. Liu, N. Qu, P. Dai, Research progress on integrated solar chimney system for freshwater production, Global Energy Interconnection, 2(3) (2019) 214-223.

[3] W. Haaf, Solar Chimneys, International Journal of Solar Energy, 2(2) (1984) 141-161.

[4] W. Haaf, K. Friedrich, G. Mayr, J. Schlaich, Solar Chimneys Part I: Principle and Construction of the Pilot Plant in Manzanares, International Journal of Solar Energy, 2(1) (1983) 3-20.

[5] R. Balijepalli, V.P. Chandramohan, K. Kirankumar, A complete design data and performance parameter evaluation of a pilot scale solar updraft tower, Heat Transfer Engineering, 41(6-7) (2020) 562-575.

[6] P. Das, V.P. Chandramohan, 3D numerical study on estimating flow and performance parameters of solar updraft tower (SUT) plant: Impact of divergent angle of chimney, ambient temperature, solar flux and turbine efficiency, Journal of Cleaner Production, 256 (2020) 120353.

[7] H. Semai, A. Bouhdjar, S. Larbi, Canopy slope effect on the performance of the solar chimney power plant, International Journal of Green Energy, 14(3) (2017) 229-238.

[8] P. Guo, Y. Zhou, D. Zhang, B. Xu, J. Li, Numerical investigation and multi-objective thermo-economic optimization of a solar chimney power plant, International Journal of Energy Research, 45(7) (2021) 10317-10331.

[9] S. Nizetic, B. Klarin, A simplified analytical approach for evaluation of the optimal ratio of pressure drop across the turbine in solar chimney power plants, Applied Energy, 87(2) (2010) 587-591.

[10] M.M. Padki, S.A. Sherif, A mathematical model for solar chimneys, in: Renewable energy, University of Joardn, 1992, pp. 289-294.

[11] N. Pasumarthi, S.A. Sherif, Experimental and theoretical performance of a demonstration solar chimney model—Part II: experimental and theoretical results and economic analysis, International Journal of Energy Research, 22(5) (1998) 443-461.

[12] A. Koonsrisuk, T. Chitsomboon, Dynamic similarity in solar chimney modeling, Solar Energy, 81(12) (2007) 1439-1446.

[13] A. Koonsrisuk, T. Chitsomboon, A single dimensionless variable for solar chimney power plant modeling, Solar Energy, 83(12) (2009) 2136-2143.

[14] A. Koonsrisuk, Mathematical modeling of sloped solar chimney power plants, Energy, 47(1) (2012) 582-589.

[15] R. Sangi, M. Amidpour, B. Hosseinizadeh, Modeling and numerical simulation of solar chimney power plants, Solar Energy, 85(5) (2011) 829-838.

[16] R. Sangi, Performance evaluation of solar chimney power plants in Iran, Renewable and Sustainable Energy Reviews, 16(1) (2012) 704-710.

[17] R. Balijepalli, V.P. Chandramohan, K. Kirankumar, Performance parameter evaluation, materials selection, solar radiation with energy losses, energy storage and turbine design procedure for a pilot scale solar updraft tower, Energy Conversion and Management, 150 (2017) 451-462.

[18] M.H. Ali, Z. Kurjak, J. Beke, Modelling and simulation of solar chimney power plants in hot and arid regions using experimental weather conditions, International Journal of Thermofluids, 20 (2023) 100434.

[19] A.P. Singh, J. Singh, A. Kumar, O.P. Singh, Vertical limit reduction of chimney in solar power plant, Renewable Energy, 217 (2023) 119118.

[20] D. Toghraie, A. Karami, M. Afrand, A. Karimipour, Effects of geometric parameters on the performance of solar chimney power plants, Energy, 162 (2018) 1052-1061.

[21] H. Nasraoui, Z. Driss, A. Ayedi, H. Kchaou, Numerical and Experimental Study of the Aerothermal Characteristics in Solar Chimney Power Plant with Hyperbolic Chimney Shape, Arabian Journal for Science and Engineering, 44(9) (2019) 7491-7504.

[22] H. Nasraoui, Z. Driss, H. Kchaou, Novel collector design for enhancing the performance of solar chimney power plant, Renewable Energy, 145 (2020) 1658-1671.

[23] A. Asnaghi, S.M. Ladjevardi, Solar chimney power plant performance in Iran, Renewable and Sustainable Energy Reviews, 16(5) (2012) 3383-3390.

[24] A.A. Sedighi, Z. Deldoost, B.M. Karambasti, Effect of thermal energy storage layer porosity on performance of solar chimney power plant considering turbine pressure drop, Energy, 194 (2020) 116859.

[25] M. RahimiLarki, R.H. Abardeh, H. Rahimzadeh, H. Sarlak, Performance analysis of a laboratory-scale tilted solar chimney system exposed to ambient crosswind, Renewable Energy, 164 (2021) 1156-1170.

[26] S. Bagheri, M. Ghodsi Hassanabad, Numerical and experimental investigation of a novel vertical solar chimney power plant for renewable energy production in urban areas, Sustainable Cities and Society, 96 (2023) 104700.

[27] D. Kumar Mandal, N. Biswas, N.K. Manna, A.C. Benim, Impact of chimney divergence and sloped absorber on energy efficacy of a solar chimney power plant (SCPP), Ain Shams Engineering Journal, 15(2) (2024) 102390.

[28] M.J. Saleh, F.S. Atallah, S. Algburi, O.K. Ahmed, Enhancement methods of the performance of a solar chimney power plant: Review, Results in Engineering, 19 (2023) 101375.

[29] A. Koonsrisuk, T. Chitsomboon, Mathematical modeling of solar chimney power plants, Energy, 51

(2013) 314-322.

[30] J.P. Pretorius, D.G. Kröger, Solar Chimney Power Plant Performance, Journal of Solar Energy Engineering, 128(3) (2006) 302-311.

[31] M. Setareh, Comprehensive mathematical study on solar chimney powerplant, Renewable Energy, 175 (2021) 470-485.

[32] S.A. Kalogirou, Solar thermal collectors and applications, Progress in Energy and Combustion Science, 30(3) (2004) 231-295.

[33] M.J. Maghrebi, R. Masoudi Nejad, S. Masoudi, Performance analysis of sloped solar chimney power plants in the southwestern region of Iran, International Journal of Ambient Energy, 38(6) (2017) 542-549.

[34] K. Rahbar, A. Riasi, Performance enhancement and optimization of solar chimney power plant integrated with transparent photovoltaic cells and desalination method, Sustainable Cities and Society, 46 (2019) 101441.

[35] M.B. Hanna, T.A.-M. Mekhail, O.M. Dahab, M.F.C. Esmail, A.R. Abdel-Rahman, Performance Investigation of the Solar Chimney Power Plants Heater Case Study in Aswan, Egypt, Journal of Power and Energy Engineering, Vol.04No.10 (2016) 22.

[36] X. Zhou, M.A.d.S. Bernardes, R.M. Ochieng, Influence of atmospheric cross flow on solar updraft tower inflow, Energy, 42(1) (2012) 393-400.

[37] X. Zhou, Y. Xu, Pressure Losses in Solar Chimney Power Plant, Journal of Solar Energy Engineering, 140(2) (2018).

[38] S.E. Haaland, Simple and Explicit Formulas for the Friction Factor in Turbulent Pipe Flow, Journal of Fluids Engineering, 105(1) (1983) 89-90.

[39] J.r. Schlaich , R. Bergermann , W. Schiel , G. Weinrebe, Design of Commercial Solar Updraft Tower Systems—Utilization of Solar Induced Convective Flows for Power Generation, Journal of Solar Energy Engineering, 127(1) (2005) 117-124.

[40] P.-h. Guo, J.-y. Li, Y. Wang, Numerical simulations of solar chimney power plant with radiation model, Renewable Energy, 62 (2014) 24-30.

HOW TO CITE THIS ARTICLE

M. Setareh, M. R. Assari, Mathematical study on performance enhancement of solar updraft tower power plant by hot gas injection from an external source, AUT J. Mech Eng., 7(3) (2023) 241-260.

DOI: 10.22060/ajme.2024.22382.6064